Proceedings of the Combustion Institute SAND2020-1224C

A comparison of the blow-out behaviour of turbulent premixed ammonia/hydrogen/nitrogen-air and methane-air flames

--Manuscript Draft--

Manuscript Number:	PROCI-D-19-00803
Article Type:	5. Turbulent Flames
Keywords:	turbulent combustion; premixed flames; Extinction; blow-out; ammonia-hydrogen-nitrogen fuel blending
Corresponding Author:	Martin Rieth Sandia National Laboratories UNITED STATES
First Author:	Samuel Wiseman
Order of Authors:	Samuel Wiseman
	Martin Rieth
	Andrea Gruber
	James Dawson
	Jacqueline Chen
Abstract:	Ammonia has been identified as a promising energy carrier that produces zero carbon dioxide emissions when used as a fuel in gas turbines. Although the combustion properties of pure ammonia are poorly suited for firing of gas turbine combustors, blends of ammonia, hydrogen, and nitrogen can be optimized to exhibit premixed, unstretched laminar flame properties very similar to those of methane. There is limited data available on the turbulent combustion characteristics of such blends and important uncertainties exist related to their blow-out behavior. The present work reports experimental measurements of the blow-out limits in an axisymmetric unconfined bluff-body stabilised burner geometry of NH3/H2/N2-air flame, comprised of 40% NH3, 45% H2, and 15% N2 by volume in the “fuel” blend. Blow-out limits for the NH3/H2/N2-air flames are compared to those of methane-air flames. Furthermore, two large-scale Direct Numerical Simulations (DNS) of temporally evolving turbulent premixed jet flames are performed to investigate differences in the turbulence-chemistry interaction and extinction behaviour between the NH 3 /H 2 /N 2 -air and methane-air mixtures. The experiments reveal that the blow-out velocity of NH3/H2/N2-air flames is an order of magnitude higher than that of methane-air flames characterized by nearly identical unstretched laminar flame speed, thermal thickness and adiabatic flame temperature. Results from the DNS support the experimental observation and clearly illustrate that a methane-air mixture exhibits a stronger tendency towards extinction compared to the NH3/H2/N2-air blend for identical strain rates. Furthermore, the DNS results reveal that, even in the presence of intense sheared turbulence, fast hydrogen diffusion into the spatially distributed preheat layers of the fragmented and highly turbulent flame front plays a crucial role in the enhancement of the local heat release rate and, ultimately, in preventing the occurrence of extinction.

A comparison of the blow-out behaviour of turbulent premixed ammonia/hydrogen/nitrogen-air and methane-air flames

Samuel Wiseman[a], Martin Rieth[b,*], Andrea Gruber[c,a], James R. Dawson[a], Jacqueline H. Chen[b]

[a] *Department of Energy and Process Engineering, Norwegian University of Science and Technology, Trondheim, Norway*
[b] *Combustion Research Facility, Sandia National Laboratories, Livermore, California*
[c] *SINTEF Energy Research, Trondheim, Norway*

Abstract

Ammonia has been identified as a promising energy carrier that produces zero carbon dioxide emissions when used as a fuel in gas turbines. Although the combustion properties of pure ammonia are poorly suited for firing of gas turbine combustors, blends of ammonia, hydrogen, and nitrogen can be optimized to exhibit premixed, unstretched laminar flame properties very similar to those of methane. There is limited data available on the turbulent combustion characteristics of such blends and important uncertainties exist related to their blow-out behavior. The present work reports experimental measurements of the blow-out limits in an axisymmetric unconfined bluff-body stabilised burner geometry of $NH_3/H_2/N_2$-air flame, comprised of 40% NH_3, 45% H_2, and 15% N_2 by volume in the "fuel" blend. Blow-out limits for the $NH_3/H_2/N_2$-air flames are compared to those of methane-air

*Corresponding Author
Email address: mrieth@sandia.gov (Martin Rieth)

flames. Furthermore, two large-scale Direct Numerical Simulations (DNS) of temporally evolving turbulent premixed jet flames are performed to investigate differences in the turbulence-chemistry interaction and extinction behaviour between the $NH_3/H_2/N_2$-air and methane-air mixtures. The experiments reveal that the blow-out velocity of $NH_3/H_2/N_2$-air flames is an order of magnitude higher than that of methane-air flames characterized by nearly identical unstretched laminar flame speed, thermal thickness and adiabatic flame temperature. Results from the DNS support the experimental observation and clearly illustrate that a methane-air mixture exhibits a stronger tendency towards extinction compared to the $NH_3/H_2/N_2$-air blend for identical strain rates. Furthermore, the DNS results reveal that, even in the presence of intense sheared turbulence, fast hydrogen diffusion into the spatially distributed preheat layers of the fragmented and highly turbulent flame front plays a crucial role in the enhancement of the local heat release rate and, ultimately, in preventing the occurrence of extinction.
Keywords: turbulent combustion, premixed flames, extinction, blow-out, ammonia-hydrogen-nitrogen fuel blending

1. Introduction

A potential shift to hydrogen as a clean energy carrier is one of the most promising strategies to significantly reduce CO_2 emissions in the face of increasing energy demand. This is particularly relevant for large-scale power generation combined with pre-combustion carbon sequestration, where large quantities of hydrogen are produced from natural gas with CO_2 capture and storage [1], as well as large-scale energy-storage schemes, where hydrogen

is produced from electrolysis by harnessing intermittent, excess power from unsteady renewable energy sources [2]. In order to simplify its transport and storage, refining hydrogen to ammonia as a carbon-free energy carrier, is a convenient alternative to liquefied hydrogen [3, 4].

The use of ammonia as a fuel for gas turbines has been explored in the past but was supplanted by conventional hydrocarbons due to its poor reactivity [5]. However, recent studies with rich-lean fuel staging have shown some promising results [4, 6]. In principle gas turbines are fuel flexible, however in reality, burner design becomes tuned to specific fuels like methane. In this paper we consider mixtures of ammonia and hydrogen, as a carbon free fuel blend, in the context of a larger industrial demonstration effort (BIGH2/Phase III - See acknowledgments). We specifically consider the partial cracking of ammonia, to form selected mixtures of ammonia, hydrogen and nitrogen that give combustion properties close to methane.

A recent numerical study, using an updated nitrogen-chemistry subset of the short San Diego mechanism in conjunction with Direct Numerical Simulation (DNS) with the S3D code [7], revealed that for nominally similar adiabatic flame temperature, thickness and propagation velocities, premixed laminar $NH_3/H_2/N_2$-air flames are significantly more resilient to extinction by strain (by a factor of five) compared with laminar CH_4-air flames in a counterflow twin-flame configuration [8].

Conditions for lean extinction or blow-out of premixed, bluff-body stabilised flames are typically characterised by the Damköhler number which relates the characteristic time-scale of the flow τ_{flow} to a chemical kinetic time scale τ_{chem} [9, 10]. However, there is a clear lack of consensus surround-

ing the appropriate choice of chemical time-scales reflecting an incomplete understanding [11]. There is more agreement that τ_{flow} scales with D/U, where D and U are characteristic length and velocity respectively, either based on residence time or strain rate [11–13] although Reynolds number effects are not well understood. A number of recent studies [12–15] have presented strong experimental evidence that along with changes to the flame topology, the frequency of localised extinction events increases as blow-out is approached.

The objective of this paper is to extend previous investigations showing the increased resilience to strain that $NH_3/H_2/N_2$-air flames exhibit relative to CH_4-air flames to turbulent flames. The present study provides both experimental evidence of increased resilience and fundamental insights provided by DNS. The fuel blend investigated is comprised of 40% NH_3, 45% H_2 and 15% N_2 by volume which approximately matches the adiabatic flame temperature, laminar flame speed and thermal thickness of CH_4-air flames under fuel-lean conditions [8]. Laboratory experiments are conducted to measure the extinction limits and planar flame topology using a simple bluff-body burner whereas two large-scale three-dimensional DNS of a temporally evolving turbulent planar jet are performed. This enables the underlying mechanisms behind the increased resilience of $NH_3/H_2/N_2$-air flames to high-levels of strain to be elucidated.

The paper is organized as follows; Sec. 2 describes the experimental methods and the DNS configuration, Sec. 3 presents the results highlighting the observed increase in blow-out limits and quantitatively illustrates the disparities in the turbulence-chemistry interactions for the different fuels followed

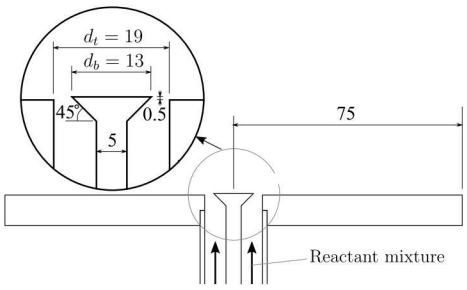

Figure 1: Sketch of burner geometry with dimensions in mm.

by conclusions in Sec. 4.

2. Experimental methodology and DNS configuration

2.1. Experiments

A schematic of the axisymmetric bluff-body burner geometry is shown in Fig. 1 that illustrates the straight injector tube with an inner diameter (d_t) of 19 mm. This is fed by a plenum comprising an expansion, a straight section with an inner diameter of 100 mm, and a contraction. Fuel and oxidant are mixed more than 2 m upstream of the plenum. The lip of the bluff-body is raised 0.5 mm above the dump plane, providing optical access to the flame base. The characteristic flow velocity, denoted U_{lip}, is the average velocity at the burner lip, estimated as $\dot{V}/A_{ann.}$, where $\dot{V}$ is the volume flow rate of reactants at standard conditions and $A_{ann.} = \pi(d_t^2 - d_b^2)/4$.

Air, methane, hydrogen, nitrogen and ammonia are supplied using Alicat mass flow controllers (MFCs) with full scale ranges from 10 slm to 2000 slm and fed into a mixing chamber upstream. The accuracy of the MFCs are 0.8% of the reading plus 0.2% of the full scale flow. For each experiment, MFCs are selected based on the required range to minimise uncertainties.

Maximum uncertainties in ϕ and U_{lip} are estimated to be ± 0.02 and 2% respectively.

Blow-out curves are measured by fixing the fuel flow rate and increasing the air flow rate. Flames are stabilised for five minutes at 90% at the estimated blow-out point. The air flow is then increased in velocity increments of 0.25% until blow-out occurs.

2.1.1. Diagnostics

A diode-pumped, frequency-doubled Nd:YAG laser (Edgewave IS 400-2-L) with a pulse energy of 10 mJ is operated at 10 kHz to pump a Sirah Credo dye laser using Rhodamine 6G dissolved in ethanol. A frequency conversion unit is used to generate a wavelength of approximately 283.55 nm with a pulse energy of 0.3 mJ.

Sheet forming optics are comprised of a pair of cylindrical lenses with focal lengths -8 mm and +100 mm. The laser sheet has a height of 35 mm at the burner axis and focuses to a width of approximately 0.2 mm at the burner axis by a plano-convex lens with a focal length of 1 m. Images are acquired at 10 kHz with a Phantom V2012 camera equipped with a LaVision IRO and a 100 mm focal length Cerco 2178 UV lens with the aperture at f/2.8. A D20-VG0035942 bandpass filter is used with a centre wavelength of 310 nm and 10 nm width (FWHM). A gate width of 80 ns is used. A frame resolution of 800×768, corresponding to a FOV of 39.6 mm by 38 mm, and a pixel resolution of 50 μm/pixel are used. Images are corrected for the background and the vertical laser sheet profile.

In order to provide an estimate of the turbulent length-scales, PIV measurements of the non-reacting flow for velocities up to 130 ms^{-1} are con-

ducted. The flow is seeded with olive oil particles. Vector calculation is done using standard correlation based methods in Davis 8.4.0 with multiple passes using 64 × 64 reducing to 32 × 32 windows with a 75% overlap. The interrogation window size is 0.896 mm.

2.2. DNS configuration

The DNS configuration corresponds to a temporally evolving turbulent planar jet flame [16–18] where two initially planar laminar flames propagate towards a temporally developing planar jet of premixed reactants at atmospheric conditions. The planar jet width is set to H=7.5 mm and the peak jet velocity to U_j=150 m/s with an initial velocity profile varying in the tranverse direction. The domain size is 16H × 10H × 12H in x (streamwise), y (transverse) and z (spanwise) directions, respectively. The grid is stretched in the y direction (only beyond ±3H which is beyond the flame and shear layer) and is uniform in the x- and z-directions. Initially, the flames are placed at y=$\pm(H + 10\tau_j s_l)$, where τ_j is the jet time defined as $\tau_j = H/U_j$ and s_l is the laminar flame speed. The initial mean jet velocity (without velocity fluctuations) (Eq.(1) in [16]) and temperature profiles are presented in Fig. 2.2. The initial mean jet velocity profile is perturbed by velocity fluctuations obtained from a synthetic Passot-Pouquet spectrum characterized by rms velocity fluctuations equal to 4% of the jet velocity and by an integral length scale of $H/3$. The initial flames are obtained from an auxiliary 1-D flame simulation evolved for several flame times and initialized by taking a 1-D steady freely propagating flame solution obtained with Cantera. The DNS cases are initialized with an equivalence ratio ϕ of 0.45 in the reactants and with a reactants' mixture temperature T_u of 750 K for both the

$NH_3/H_2/N_2$ (40%/45%/15% by volume) fuel blend and the CH_4 mixture. At these conditions, the laminar flame thickness (δ_l), laminar flame speed (s_l), laminar flame time (τ_l) are, respectively: 524 μm, 0.8568 m/s, 612 μs for the $NH_3/H_2/N_2$ blend and 540 μm, 0.8622 m/s, 626 μs for methane. Identical values for H and U_j are used for both cases, leading to slightly different Reynolds numbers of 13800 ($NH_3/H_2/N_2$) and 14800 (CH_4) and jet Damköhler numbers ($Da_{jet} = t_j/(\delta_l s_l^{-1})$) of 0.082 ($NH_3/H_2/N_2$) and 0.08 ($CH_4$). The resolution is set such that there are at least 14 grid points within the laminar thermal flame thickness (i.e., Δ=37.4μm). This leads to a grid of 3456 $\times$ 1280 $\times$ 2560 points with approximately 11 billion grid points. The simulations are performed on 900 heterogeneous nodes on the Oak Ridge National Laboratory Summit supercomputer, employing Nvidia Volta GPUs (6 on each node). The simulations require wall times of approximately 79 h ($NH_3/H_2/N_2$) and 67 h (CH_4) for 10 t_j. The S3D-Legion DNS code [19, 20] is employed in the present study. This is a portable high-performance version of the S3D DNS code [7] based on the asynchronous dynamic task-based Legion programming system and runtime [21]. The recently updated nitrogen-chemistry subset of the San Diego mechanism [8] is ported to the S3D-Legion framework and used for the DNS of the $NH_3/H_2/N_2$-air turbulent premixed flame flame while the short mechanism by Smoke and Giovangigli [22] is used for the methane-air flame.

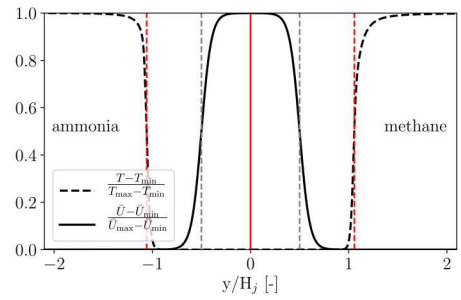

Figure 2: Initial normalized temperature and mean velocity profiles (excluding fluctuations). The left side shows the profile for $NH_3/H_2/N_2$, the right side shows the profile for CH_4 (both profiles are symmetrical). Grey dashed lines: locations of the initial shear layer $\pm$H/2. Red dashed lines: initial flame locations $\pm(H + 10t_j s_l)$.

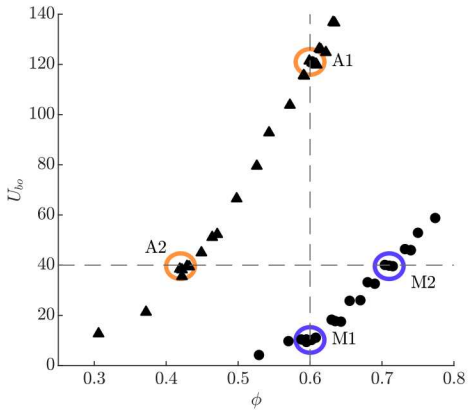

Figure 3: Measured blow-out curves for the $NH_3/H_2/N_2$blend (triangles) and CH_4 (circles). Labelled points are discussed in the text.

3. Results

3.1. Blow-out curves and Damköhler criteria

Figure 3 plots the measured blow-out curves for both CH_4-air and $NH_3/H_2/N_2$-air flames. The experimental results very clearly reveal that the blow-out velocities of the $NH_3/H_2/N_2$-air flames are much greater than the CH_4-air

flames for all equivalence ratios investigated in this study. The maximum ϕ at which the blow-out velocity could be measured for the $NH_3/H_2/N_2$ flames is limited by the maximum air flow rate available in the laboratory. We now focus on a comparison between the flames at points A1 and M1 (marked in Fig. 3) at $\phi = 0.6$ which have approximately matched laminar flame properties, $S_{L,0}$, δ_{th} and T_{ad} and flames A2 and M2 which blow-out at the same velocity, $U_{bo} = 40$ ms^{-1}. Table 1 shows the laminar flame properties and chemical kinetic time scales for the four flames obtained from Cantera simulations. The time-scales are for a perfectly stirred reactor, τ_{psr}, inverse of the extinction strain rate, $\tau_{ext} = 1/\kappa_{ext}$, and the laminar flame time, $\tau_{pf} = \delta_{th}/S_{L,0}$. An estimate of the effective Lewis number was evaluated using a heat release weighted formulation (Le_q) [23] and a diffusion-weighted formulation (Le_D) [24]. The flames at M1 and A1 show an order of magni-

Case	**M1**	**A1**	**M2**	**A2**
$S_{L,0}$ (cm/s)	11.8	12.6	21.5	1.8
δ_{th} (mm)	0.98	1.02	0.67	3.6
T_{ad} (K)	1667	1633	1875	1350
τ_{psr} (ms)	0.34	0.13	0.13	1.48
τ_{ext} (ms)	1.75	0.46	0.75	4.46
τ_{pf} (ms)	8.32	8.19	2.87	370.8
$Le_q(Le_D)$	0.98	0.86 (0.53)	0.98	0.82 (0.50)

Table 1: Computed reaction mixture properties for the points indicated in Fig. 3.

tude difference in the blow-out velocity even though the unstretched laminar flame properties are all within 10%. Although τ_{psr} and $\tau_{ext} = 1/\kappa_{ext}$ differ by up to a factor of 4, it does not explain a factor of 12 difference in U_{bo}. On the other side, flames A2 and M2 both blow-out at the same velocity,

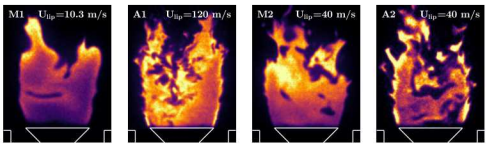

Figure 4: OH PLIF images of flames 1 s before blow-out.

$U_{bo} = 40$ ms^{-1} and, therefore, approximately at the same Reynolds numbers. However, values for τ_{psr}, τ_{ext}, or τ_{pf} for M2 in Table 1 are an order of magnitude lower than for A2 suggesting, contrary to the present observation, a much greater resistance to blow-out.

Clearly, laminar flame properties, conventionally used in similar contexts, seem unable to explain the present observations. Further information can be obtained by considering the flame topology close to blow-out, as shown in Figure Fig. 4. The left panels shows flames M1 and A1. It is evident that the flame surface of A1 (the $NH_3/H_2/N_2$-air flame) is visibly more turbulent than M1, as shown by the degree of wrinkling at the flame edge. The estimated turbulent Reynolds numbers are $Re_t = u'l_t/\nu_0 = 97$ and 1100, respectively. A closer inspection shows that for the methane-air flame, M1, the intensity of the OH signal has minimum values close to the bluff-body, a qualitative indication of reduced heat release rate most likely due to relatively high levels of strain at the burner exit. The magnitude of the heat release increases downstream reaching a maximum near the top of the flame. This is consistent for flames with $Le > 1$ where the consumption speed and the flame temperature decrease in response to strain, eventually leading to local extinction. In contrast, the $NH_3/H_2/N_2$-air flame, A1, has a much greater $Re_t = u'l_t$ and is much more broken-up and fragmented, yet everywhere along the flame edge there are local regions of high heat release rate, even

at the base of the flame near the bluff body. The observed high levels of OH concentration are consistent with $Le < 1$ flames, as aerodynamic strain increases the consumption speed and burned gas temperature [25, 26]. It is conjectured that, in this case, the observed flame behavior is caused by fast hydrogen diffusion towards the hot regions of the flow. Similar comparisons can be drawn between flames M2 and A2 shown in the right panels of Fig. 4.

In summary, the present experimental observations show that laminar flame properties, even if scaled to take into account the presence of turbulence, are unable to account for the measured order of magnitude increase in the blow-out velocity for $NH_3/H_2/N_2$-air flames. Analysis of DNS data for highly-strained, turbulent premixed $NH_3/H_2/N_2$-air and CH_4-air flames in the next section provides a more detailed understanding of the underlying physical mechanisms that may underly the different blow-out behaviors.

.

3.2. Turbulence-chemistry interaction and extinction behavior

The two DNS cases were analyzed and compared at a time $t/t_j \approx 21$ which is close to the time of maximum turbulent flame surface area generated by the interaction of the laminar premixed flames with the sheared turbulence. At this time, the flames appear highly wrinkled, and whereas significant amounts of flame-flame interaction due to self propagation and strain rate have occurred on both sides of the planar jet, significant interaction with flames from opposite sides of the jet has not occurred yet, particularly for the methane-air flame. Figure 5 shows the instantaneous heat release rate, and the OH mass fraction in a representative xy-plane, normalized by the maximum values observed in the laminar unstrained $NH_3/H_2/N_2$-air and

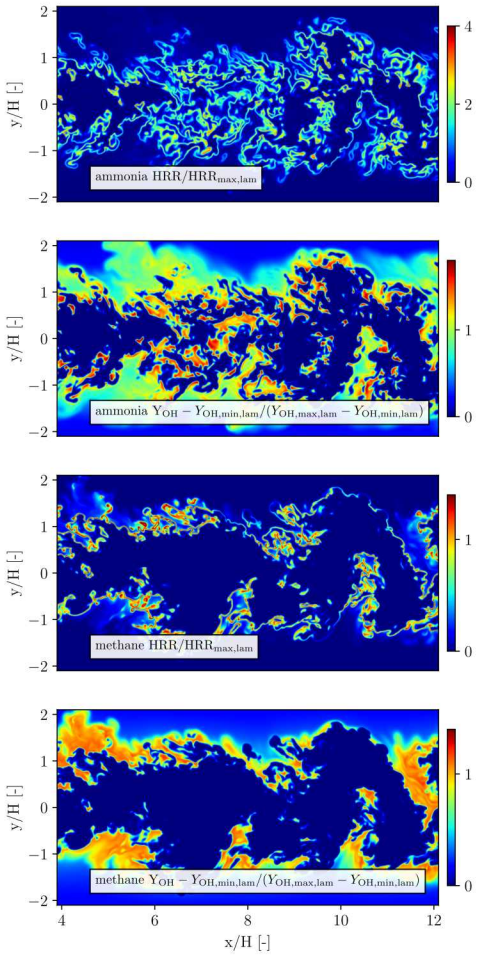

Figure 5: Normalized heat release rate and OH mass fraction at $t/t_j \approx 21$ for the $NH_3/H_2/N_2$blend (upper) and CH_4 (lower). The maximum values of laminar unstrained flames are used for normalization. The region of the domain shown is truncated in the x and y directions.

CH_4-air flames, respectively, at a time of $t/t_j \approx 21$. The $NH_3/H_2/N_2$-air flame is burning much more strongly than the methane-air flame as indicated by larger values of the nondimensional heat release rates. In addition, the $NH_3/H_2/N_2$-air flame exhibits a greater degree of flame wrinkling and

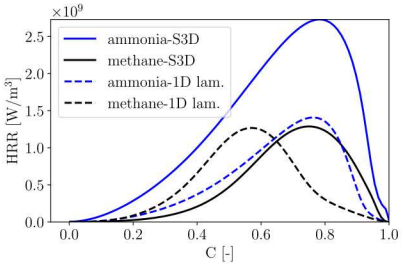

Figure 6: Heat release rate versus progress variable at $t/t_j \approx 21$. Laminar unstrained flame solutions are shown for reference.

a much larger flame surface area, whereas the CH_4-air flame exhibits local extinction or partial-extinction appearing as disruptions (or significant decrease in intensity) to the OH and heat release rate layers. The increase in the burning rate is further substantiated by examining the conditional mean of the heat release rate conditioned on the progress variable shown in Fig. 6. The progress variable C is based on the mass fraction of H_2O, normalized by the burnt and unburnt values in the respective laminar unstrained flames. In the figure the conditional mean of the turbulent heat release rate profile for the turbulent CH_4-air flame shows a lower peak compared with unstrained laminar conditions and a shift towards higher values of the progress variable characteristic of highly strained laminar flames [27]. The peak heat release rate of the $NH_3/H_2/N_2$-air flame significantly exceeds the peak at laminar conditions, and significant heat release rate extends far towards low values of the progress variable. This is in accordance with observations, from strained laminar premixed flames, in which the $NH_3/H_2/N_2$-air flame shows a strong correlation between the peak heat release rate and high values of strain rate. Though not shown here, a stronger increase in heat release rate with strain

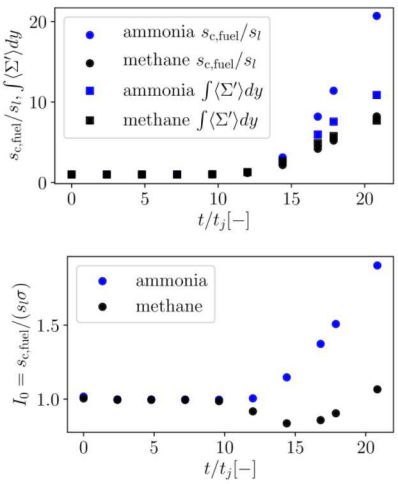

Figure 7: Temporal evolution of the normalized fuel consumption speed and flame surface area ratio (top), and ratio of turbulent to laminar burning rate per unit area (bottom) for $NH_3/H_2/N_2$blend and CH_4.

is found for the $NH_3/H_2/N_2$-air flame compared to pure ammonia-air or pure hydrogen-air flames.

Figure 7 presents the fuel consumption rate and the flame surface area ratio calculated as $s_{c,fuel} = (\rho_u(Y_{fuel,b} - Y_{fuel,u}))^{-1} \int_0^{L_y} \langle\omega_{fuel}\rangle$ dy, with ρ_u being the density in the unburnt gas, $Y_{fuel,b}$ and $Y_{fuel,u}$ the fuel mass fraction in the burnt and unburnt gas, respectively, and $\langle\omega_{fuel}\rangle$ the net fuel production rate averaged in the homogeneous x- and z-directions. The flame surface area ratio is calculated as $\sigma = \int_0^{L_y} \langle\Sigma'\rangle dy$, with $\langle\Sigma'\rangle$ being the averaged flame surface density $\Sigma' = |\nabla C|$. The turbulent $NH_3/H_2/N_2$-air flame shows a much stronger increase in fuel consumption speed compared to the methane-air flame. In addition, the fuel consumption speed increases more strongly than the flame surface area ratio for the $NH_3/H_2/N_2$-air flame, and less strongly for methane-air flame. This is further illustrated in Fig. 7 (bottom)

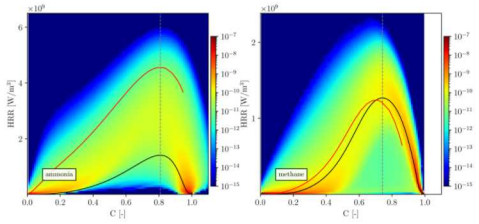

Figure 8: Joint PDF of heat release rate and progress variable for the $NH_3/H_2/N_2$blend (left) and CH_4 (right) DNS cases. Lines: laminar unstrained flame (black), strained laminar flame near extinction (red), progress variable at unstrained maximum laminar heat release (gray).

showing that the ratio of the turbulent to laminar burning rate per unit area increases for the $NH_3/H_2/N_2$-air flame and decreases for the methane-air flame. This, ultimately indicates that while the methane-air flame is weakened by the strong turbulence, the $NH_3/H_2/N_2$-air flame is strengthened by it.

Figure 8 illustrates the joint probability density functions of the heat release rate and progress variable at $t/t_j \approx 21$. In addition, profiles for laminar unstrained and strained flames close to extinction are shown. The heat release rate for the $NH_3/H_2/N_2$-air flame is significantly broader, which is consistent with the laminar behavior under the influence of strain. The $NH_3/H_2/N_2$-air flame shows very low probabilities for heat release rates lower than that of the laminar unstrained flame, whereas the methane-air flame shows a significant probability of low heat release compared to the laminar solutions, further indicating the occurrence of localized partial-extinction. As anticipated in the previous section, a viable hypothesis that can explain why the $NH_3/H_2/N_2$-air flame is much more resilient to strain is the occurrence of fast hydrogen diffusion (preferential diffusion), locally increasing the burning

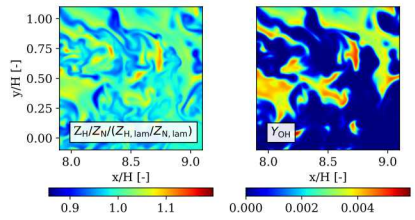

Figure 9: Ratio of H to N element mass fractions and OH mass fraction for the ammonia-hydrogen blend case.

intensity and amplified by turbulent stretch. The DNS results support this hypothesis, and this is is shown in Fig. 9, where high H to N elemental mass ratio, i.e., regions of preferential hydrogen diffusion, coincide with regions of high values for the OH mass fraction, a clear consequence of intense burning and high heat release rate (not shown).

4. Conclusions

A joint experimental and numerical study was conducted of the blow-out behaviour of $NH_3/H_2/N_2$-air flames, blended such that the flame exhibits similar premixed, unstretched laminar flame properties as lean methane-air flames. In the experiment, blow-out curves for the ammonia blend and methane-air flames were measured in an axisymmetric, unconfined, bluff-body stabilised burner, showing an order of magnitude difference in blow-out velocity. DNS in a temporally-evolving slot jet configuration provide further understanding of the differences in behavior of $NH_3/H_2/N_2$-air and methane-air flames in highly strained turbulent conditions. The $NH_3/H_2/N_2$-air flame exhibits a much stronger increase in flame surface area and fuel consumption rate than the methane-air flame. The analysis revealed that

the $NH_3/H_2/N_2$-air flame exhibits strongly enhanced heat release rates compared to a methane-air flame and points towards preferential diffusion of hydrogen as the main reason for increased burning rates. Future work will focus on understanding the effects of pressure on the resilience of flames with ammonia blends and on nitric oxide generation.

Acknowledgments

The present research is supported by the CLIMIT-Demo program of the Research Council of Norway, Project Number 617137, BIGH2/Phase III and by UNINETT Sigma2 Project Number nn9527k. Support for the Sandia authors was provided by the U.S. Department of Energy, Office of Vehicle Technologies and by the U.S. Army Research Laboratory. Sandia National Laboratories is a multimission laboratory managed and operated by National Technology and Engineering Solutions of Sandia, LLC., a wholly owned subsidiary of Honeywell International, Inc., for the U.S. Department of Energy's National Nuclear Security Administration under contract DE-NA-0003525.

References

[1] H. F. Abbas, W. M. A. Wan Daud, Hydrogen production by methane decomposition: a review, International journal of hydrogen energy 35 (2010) 1160–1190.

[2] A. Ursua, L. M. Gandia, P. Sanchis, Hydrogen production from water electrolysis: current status and future trends, Proceedings of the IEEE 100 (2011) 410–426.

[3] J. Fuhrmann, M. Hulsebrock, U. Krewer, Transition to renewable energy systems, D. Stolten and V. Scherer, Wiley-VCH Verlag GmbH & Co. KGaA, 2013, pp. 691–706.

[4] H. Kobayashi, A. Hayakawa, K. Somarathne, E. Okafor, Science and technology of ammonia combustion, Proceedings of the Combustion Institute 37 (2019) 109 – 133.

[5] F. Verkamp, M. Hardin, J. Williams, Ammonia combustion properties and performance in gas-turbine burners, in: Symposium (International) on Combustion, volume 11, Elsevier, 1967, pp. 985–992.

[6] A. Valera-Medina, H. Xiao, M. Owen-Jones, W. David, P. Bowen, Ammonia for power, Progress in Energy and Combustion Science 69 (2018) 63 – 102.

[7] J. H. Chen, A. Choudhary, B. de Supinski, M. DeVries, E. R. Hawkes, S. Klasky, W. K. Liao, K. L. Ma, J. Mellor-Crummey, N. Podhorski, R. Sankaran, S. Shende, C. S. Yoo, Terascale direct numerical simulations of turbulent combustion using s3d, Computational Science and Discovery 2 (2009) 1–31.

[8] Y. Jiang, A. Gruber, K. Seshadri, F. A. Williams, An updated short chemical-kinetic nitrogen mechanism for carbon-free combustion applications, International Journal of Energy Research in press (2019).

[9] A. Mellor, Semi-empirical correlations for gas turbine emissions, ignition, and flame stabilization, Progress in Energy and Combustion Science 6 (1980) 347 – 358.

[10] K. Radhakrishnan, J. B. Heywood, R. J. Tabaczynski, Premixed turbulent flame blowoff velocity correlation based on coherent structures in turbulent flows, Combustion and Flame 42 (1981) 19 – 33.

[11] S. J. Shanbhogue, S. Husain, T. Lieuwen, Lean blowoff of bluff body stabilized flames: Scaling and dynamics, Progress in Energy and Combustion Science 35 (2009) 98 – 120.

[12] S. Chaudhuri, S. Kostka, M. W. Renfro, B. M. Cetegen, Blowoff dynamics of bluff body stabilized turbulent premixed flames, Combustion and Flame 157 (2010) 790 – 802.

[13] B. R. Chowdhury, B. M. Cetegen, Effects of free stream flow turbulence on blowoff characteristics of bluff-body stabilized premixed flames, Combustion and Flame 190 (2018) 302 – 316.

[14] J. Kariuki, A. Dowlut, R. Yuan, R. Balachandran, E. Mastorakos, Heat release imaging in turbulent premixed methane–air flames close to blow-off, Proceedings of the Combustion Institute 35 (2015) 1443 – 1450.

[15] J. Kariuki, A. Dowlut, R. Balachandran, E. Mastorakos, Heat release imaging in turbulent premixed ethylene-air flames near blow-off, Flow, Turbulence and Combustion 96 (2016) 1039–1051.

[16] E. R. Hawkes, R. Sankaran, J. C. Sutherland, J. H. Chen, Scalar mixing in direct numerical simulations of temporally evolving plane jet flames with skeletal co/h2 kinetics, in: Proceedings 31th International Symposium on Combustion, The Combustion Institute, 2007, pp. 1633–1640.

[17] E. Hawkes, O. Chatakonda, H. Kolla, A. Kerstein, J. Chen, A petascale direct numerical simulation study of the modelling of flame wrinkling for large-eddy simulations in intense turbulence, Combustion and Flame 159 (2012) 2690–2703.

[18] P. Trisjono, H. Pitsch, A direct numerical simulation study on no formation in lean premixed flames, Proceedings of the Combustion Institute 36 (2017) 2033 – 2043.

[19] S. Treichler, M. Bauer, A. Bhagatwala, G. Borghesi, R. Sankaran, H. Kolla, P. S. McCormick, E. Slaughter, W. Lee, A. Aiken, J. H. Chen, Exascale Scientific Applications: Scalability and Performance Portability, Chapman and Hall/CRC, 2017.

[20] G. Borghesi, A. Krisman, T. Lu, J. H. Chen, Direct numerical simulation of a temporally evolving air/n-dodecane jet at low-temperature diesel-relevant conditions, Combustion and Flame 195 (2018) 183 – 202. Special Commemorative Issue: Professor Chung King (Ed) Law 70th Birthday.

[21] M. Bauer, S. Treichler, E. Slaughter, A. Aiken, Legion: Expressing locality and independence with logical regions, in: Proceedings of the International Conference on High Performance Computing, Networking, Storage and Analysis, SC '12, IEEE Computer Society Press, Los Alamitos, CA, USA, 2012, pp. 66:1–66:11.

[22] M. Smoke, V. Giovangigli, Reduced Kinetic Mech- anisms and Asymptotic Approximations for Methane-Air Flames, Springer, 1991, pp. 1–28.

[23] C. Law, G. Jomaas, J. Bechtold, Cellular instabilities of expanding hydrogen/propane spherical flames at elevated pressures: theory and experiment, Proceedings of the Combustion Institute 30 (2005) 159 – 167.

[24] F. Dinkelacker, B. Manickam, S. Muppala, Modelling and simulation of lean premixed turbulent methane/hydrogen/air flames with an effective lewis number approach, Combustion and Flame 158 (2011) 1742 – 1749.

[25] C. K. Law, Combustion Physics, Cambridge University Press, 2006.

[26] T. Poinsot, D. Veynante, Theoretical and Numerical Combustion, second ed., Edwards, 2005.

[27] P. A. Libby, A. Linan, F. A. Williams, Strained premixed laminar flames with nonunity lewis numbers, Combustion Science and Technology 34 (1983) 257–293.